

## Anisotropy at high temperatures

Y.T. Keum\* and B.Y. Ghoo

Ceramic Processing Research Center (CPRC), Hanyang University, Seoul 133-791, Korea

In this study, special attention is paid to the definition of planar anisotropy of non-ferrous sheets at high temperatures. Barlat's strain potential is employed for depicting the yield behavior. A smoothing function with a third order polynomial is introduced for non-isothermal Barlat's anisotropy coefficients. The predicted Barlat's coefficients are compared with experimentally obtained coefficients. As a crucial result, the smoothing function provides a big advantage in evaluating non-isothermal Barlat's anisotropy coefficients: there is no necessity to carry out tensile tests in high temperatures.

**Key words:** Anisotropy, Barlat's Yield Function, Constitutive Equation, High Temperature, Non-isothermal Forming.

### Introduction

Forming technology at high temperatures, typically at or above about  $0.5T_m$  where  $T_m$  is the absolute melting point, has received considerable attention over a period of many years. Currently, increasing interest in non-isothermal forming for non-ferrous sheets is being driven by weight-reduction trends as well as precision forming technology. However, non-isothermal sheet forming, is so difficult, unsettled and complex that extensive trials are required, which involve substantial time and cost. Therefore, the need for numerical analysis of forming processes for non-ferrous materials becomes more important for many industries.

Since the work of Bishop [1] on a numerical method for solving thermo-plasticity problems, many studies on thermo-plasticity have been carried out. However, it is very difficult to find examples of successful 3-dimensional forming analysis of an arbitrary shape for a non-ferrous sheet because the anomalous behavior of the non-ferrous sheet is very complex and irregular [2]. Some outstanding non-quadratic planar anisotropic yield criteria were reported and have been applied to describe the anomalous behavior of non-ferrous sheets [3-5]. Although the results in the planar anisotropy discussed above are interesting, little effort has been expended to model the coupled effects of heat and planar anisotropy. Hence, it is very difficult to find examples in which finite element analyses were carried out for the non-isothermal forming of non-ferrous sheets. For steel or stainless steel sheets, however, a large number of experimental, analytical, and numerical studies, from quite simple to very sophisticated ones, have been reported on non-isothermal forming techno-

logy. Especially, a constitutive relation in the non-isothermal forming analysis affects the accuracy of the analysis result so much that many studies have been performed on this problem [6, 7].

In the present study, the non-isothermal constitutive relation and planar anisotropy of nonferrous sheets are investigated for numerical simulation. Smoothing functions with the third order polynomial are introduced to describe non-isothermal Barlat's anisotropy coefficients. The coefficients predicted by smoothing functions are compared with those found by experimental measurements.

### Planar Anisotropy

In order to define the anisotropy of non-ferrous sheets, the yield function and associated flow rule, constitutive equation, and other material properties should be specified. In this study, the Barlat's strain potential is used for a description of yield behavior.

#### Barlat's anisotropic yield criterion

Barlat's strain rate potential [4] is employed for the plastic anomalous behavior of non-ferrous sheets. In Barlat's anisotropic criterion, the strain rate potential  $\Psi$  is defined as follows:

$$\Psi(D_i) = |D_1|^M + |D_2|^M + |D_1 + D_2|^M = 2\dot{\epsilon}_e^M \quad (1)$$

where  $D_{k=1,2}$  are the principal values of a symmetric matrix  $\mathbf{L}$ ,

$$\mathbf{L} = \begin{bmatrix} \frac{(2c_2 + c_3)\dot{\epsilon}_{11} + (c_2 - c_3)\dot{\epsilon}_{22}}{3} & c_6\dot{\epsilon}_{12} \\ c_6\dot{\epsilon}_{12} & \frac{(c_1 - c_3)\dot{\epsilon}_{11} + (2c_1 + c_3)\dot{\epsilon}_{22}}{3} \end{bmatrix} \quad (2)$$

\*Corresponding author:  
Tel : +82-2-2290-0436  
Fax : +82-2-2298-6194  
E-mail: ytkeum@hanyang.ac.kr

In Eq. (1), the effective strain rate,  $\dot{\epsilon}_e$ , is defined as the positive strain rate for plane strain tension in the direction 1. The recommended values of exponent  $M$  are  $M=4/3$  for FCC materials and  $M=3/2$  for BCC materials. In Eq. (2), the Barlat's anisotropy coefficients,  $c_{i=1,2,3,6}$ , can be obtained from experimental data such as directional plastic strain ratios, yield stresses, shear stresses, etc.

### Anisotropy coefficients at high temperatures

At the melting temperature  $T_m$  of a non-ferrous sheet, Barlat's anisotropy coefficients are assumed to be 1 because of the material isotropy. Barlat's anisotropy coefficients approach 1 as the temperature increases to the melting temperature. Furthermore, at temperature  $\omega T_m$ , where  $\omega$  is a scale factor that ranges from 0 to 1, the sheet may be quasi-isotropic and the material starts to become isotropic. When  $\omega$  is equal to 0, the sheet is isotropic at all temperatures. Since the non-ferrous sheet is a compound material whose melting point has a range from solidus to liquidus temperatures, the quasi-isotropic temperature can be assumed as the solidus temperature. In general,  $\omega$  is about 0.9-0.95 when the temperature is at the liquidus. Four control points can then be considered to determine the Barlat's anisotropy coefficients associated with various temperatures: room temperature (RT), quasi-isotropic temperatures ( $\omega T_m$ ), melting temperature ( $T_m$ ), and midpoint temperature between  $\omega T_m$  and  $T_m$  ( $(\omega T_m + T_m)/2$ ). Smoothing functions,  $d_i$ , for non-isothermal Barlat's anisotropy coefficients may now be defined with a polynomial form as follows:

$$d_i = a_{0i} + a_{1i}T + a_{2i}T^2 + a_{3i}T^3 \quad (3)$$

where  $a$ =constants determined from four control points. Figure 1 helps to understand the smoothing functions. In Fig. 1,  $d_1$  and  $d_2$  are smoothing functions to determine the Barlat's anisotropy coefficients associated with the temperatures whose values at room temperature are

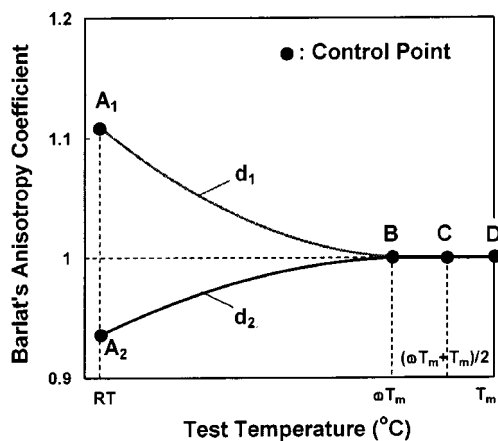


Fig. 1. Smoothing functions for determining Barlat's anisotropy coefficients.

greater and less than 1, respectively. A smoothing function,  $d_i$ , is derived using 4 control points, A, B, C, and D. As a consequence, the non-isothermal Barlat's anisotropy coefficients can be determined using those of room temperature only.

### Constitutive equation

It is well known that strain rate is one of the main factors affecting the constitutive behaviors of strain at high temperatures. Hence, in order to generate a more accurate constitutive relation incorporating the simultaneous effects of strain, strain rate and temperature on a flow stress, the following constitutive equation is used:

$$\bar{\sigma} = \sigma_0(T) + K(T) \times (\bar{\epsilon} + \epsilon_0(T))^{n(T)} \times (\dot{\bar{\epsilon}}/\gamma(T))^{m(T)} \quad (4)$$

where  $\sigma_0(T)$ =pre-stress;  $\epsilon_0(T)$ =pre-strain;  $\gamma(T)$ =base strain rate;  $K(T)$ =strength coefficient;  $n(T)$ =work-hardening exponent;  $m(T)$ =strain rate sensitivity. They are first determined by the least-square analysis at each temperature and then regressed by polynomial functions with respect to the temperature,  $T$ .

### Application

The theories proposed in this study are applied to AL5052 sheet to show the reliability. Then analytical results found by current theory are compared with those obtained from experimental measurements.

The true stress-strain curves of AL5052 sheet associated over the temperature range from 18°C to 350°C are shown in Fig. 2, in which the stress-strain points experimentally measured are analytically interpolated with Eq. (4). The material constants firstly determined by the least-square analysis at each temperature and then regressed by fourth or fifth order polynomial functions with respect to the temperature are listed in Table 1. It is seen that, as the test temperature rises, the tensile stress decreases, whereas elongation increases: the elongation and tensile stress at 300°C are respec-

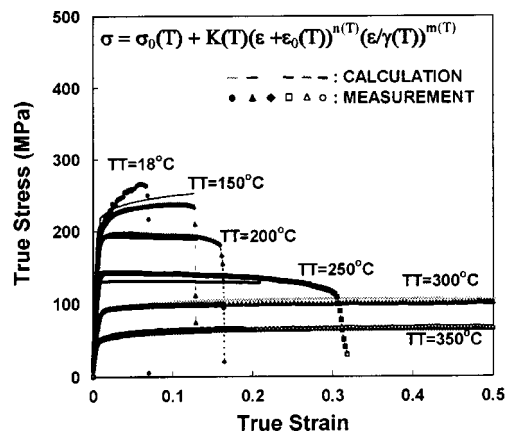
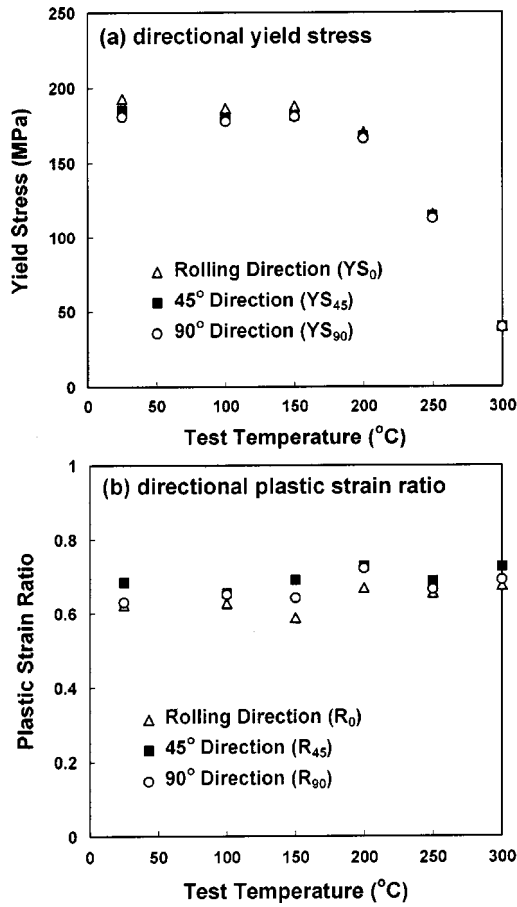


Fig. 2. Stress-strain curves of AL5052 aluminum-alloy sheet at various test temperatures.

**Table 1.** Material constants of AL5052 aluminum-alloy sheet

Material Constant	Function or Value
$K(T)$ [Mpa]	$-3.96e^2+2.47T-4.70e^{-2}T^2+2.27e^{-4}T^3$ $-4.74e^{-7}T^4+3.72e^{-10}T^5$
$n(T)$	$-1.41e^{-1}+2.28e^{-3}T-4.97e^{-5}T^2-2.96e^{-7}T^3$ $-7.65e^{-10}T^4+7.87e^{-13}T^5$
$m(T)$ [1/s]	$-8.00e^{-4}+2.91e^{-4}T-1.58e^{-5}T^2-2.29e^{-7}T^3$ $-9.02e^{-10}T^4+1.11e^{-12}T^5$
$\sigma_0(T)$ [MPa]	$1.99e^3-2.28e^1T+8.93e^{-2}T^2$ $-1.43e^{-4}T^3+8.04e^{-8}T^4$
$\epsilon_0(T)$	0.0001
$\gamma(T)$ [1/s]	1.0



**Fig. 3.** (a) Directional yield stress and (b) directional plastic strain ratio of AL5052 sheet as functions of test temperature.

tively 99% and 88MPa, while they are 7.3% and 232 MPa at room temperature. The formability of AL5052 sheet seems to be remarkably enhanced as the temperature rises.

The directional yield stress and plastic strain ratio of AL5052 sheet are shown in Fig. 3. The values of yield stress vary strongly with test temperature, while those of plastic strain ratio vary only slightly. In both yield stress and plastic strain ratio, however, the directional characteristics vary little with test temperature change.

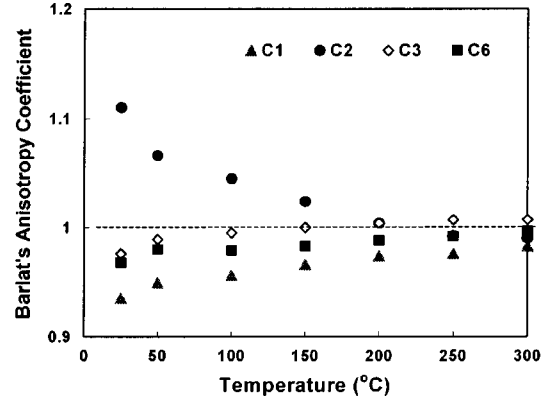


**Fig. 4.** Barlat's anisotropy coefficients for AL5052 aluminum-alloy sheet as a function of test temperature.

Therefore, it is assumed that the directional characteristics at room temperature are maintained regardless of the temperature.

The anisotropy coefficients of Barlat's strain rate potential are determined using the yield stresses and plastic strain ratios in 3 directions shown in Fig. 3 using the method proposed by Keum and Lee [8]. In Fig. 4, Barlat's anisotropy coefficients approach 1 as the test temperature rises. It is inferred that Barlat's anisotropy coefficients at the melting temperature become 1, which corresponds to the isotropic state as the assumption discussed in the previous section. Employing the Barlat's anisotropy coefficients at room temperature, 18°C, in this study, and those of 3 more control points, the smoothing functions,  $d_i$ , are derived and shown in Fig. 5 together with those of Fig. 4. In Fig. 5, "prediction" means the Barlat's anisotropy coefficients obtained from the smoothing functions and "experiment" means those calculated using the yield stresses

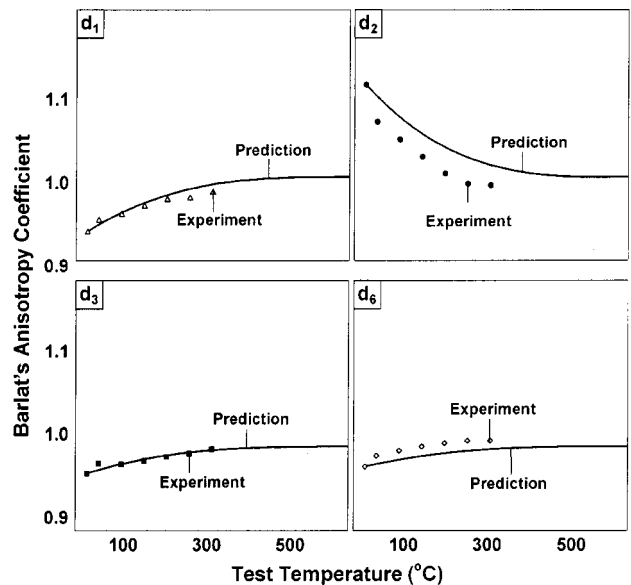


**Fig. 5.** Comparison of predicted and experimental Barlat's anisotropy coefficients.

and plastic strain ratios in 3 directions. In this study,  $\omega=0.91$  is chosen from the assumption that quasi-isotropy occurs at the solidus temperature of 593 where the melting temperature,  $T_m$ , is the liquidus, 649°C. In the comparison between prediction and experiment, there are some deviations generally similar trends. Even though some deviations are unavoidable in the accuracy, this smoothing function provides a significant advantage for non-isothermal numerical analysis. It is not necessary to carry out non-isothermal tensile tests.

### Conclusion

In order to analyze the non-isothermal forming of non-ferrous sheets with planar anisotropy, the anisotropic behavior at high temperature was investigated. The conclusions derived through this study are summarized as follows: Third order polynomial smoothing functions for describing non-isothermal Barlat's anisotropy coefficients provide a big advantage in non-isothermal forming analyses. It is not necessary to carry out high temperature tensile tests to determine non-isothermal Barlat's anisotropy coefficients.

### Acknowledgment

This work was supported by the Korea Science and Engineering Foundation (KOSEF) through the Ceramic Processing Research Center at Hanyang University.

### References

1. Barlat, F. and Chung, K., Anisotropic Potentials for

- Plastically Deforming Metals, Modeling and Simulation in Material Science and Engineering 1 (1991) 403-416.
2. Barlat, F. Lege, D.J. Berm, J.C. and Warren, C.J., Constitutive Behavior for Anisotropic Materials and Application to a 2090 Al-Li Alloy. In T.C. Lowe (ed.), Modeling the Deformation of Crystalline Solids (1991) 189-203.
  3. Bishop, J.F.W., An Approximate Method for Determining the Temperatures Reached in Steady Motion Problems of Plane Plastic Strain, Quarterly Journal of Mechanics and Applied Mathematics 9 (1956) 236-246.
  4. Charles, J.F. Habraken, A.M. and Lecomte, J., Modeling of Elasto-visco-plastic Behavior of Steels at High Temperatures, Simulation of Materials Processing: Theory, Methods and Applications (NUMIFORM98). Heutink, J. & Baaijens, F.P.T. Eds. Balkema, Rotterdam (1998) 277-282.
  5. Hill, R., Constitutive Modeling of Orthotropic Plasticity in Sheet Metals, Journal of Mechanics and Physics of Solids 38 (1990) 405-417.
  6. Keum, Y.T. and Lee, G.B., Sectional Finite Element Analysis of Forming Processes for Aluminum-alloy Sheet Metals, International Journal of Mechanical Science 42(10) (2000) 1911-1933.
  7. Lee, S.Y. Keum, Y.T. Park, J.M. Chung, K. and Barlat, F., Three-Dimensional Finite Element Method Simulations of Stamping Processes of Planar Anisotropic Sheet Metals, International Journal of Mechanical Science 39 (1997) 1181-1198.
  8. Pietrzyk, M. and Kedzierski, Z., Inverse Analysis Applied to the Evaluation of Rheological and Microstructural Parameters in Hot Forming of Steels, Simulation of Materials Processing: Theory, Methods and Applications (NUMIFORM98). Heutink, J. & Baaijens, F.P.T. Eds. Balkema, Rotterdam (1998) 163-168.
  9. Woodthorpe, J. and Pearce, R., The Anomalous Behavior of Aluminum Sheet under Balanced Biaxial Tension, International Journal of Mechanical Science 12 (1970) 341-347.